FORCE RELAXATION AND PERMANENT DEFORMATION OF ERYTHROCYTE MEMBRANE

D. R. MARKLE, E. A. EVANS, AND R. M. HOCHMUTH
Department of Biomedical Engineering, Duke University, Durham, North Carolina

ABSTRACT Force relaxation and permanent deformation processes in erythrocyte membrane were investigated with two techniques: micropipette aspiration of a portion of a flaccid cell, and extension of a whole cell between two micropipettes. In both experiments, at surface extension ratios <3:1, the extent of residual membrane deformation is negligible when the time of extension is less than several minutes. However, extensions maintained longer result in significant force relaxation and permanent deformation. The magnitude of the permanent deformation is proportional to the total time period of extension and the level of the applied force. Based on these observations, a nonlinear constitutive relation for surface deformation is postulated that serially couples a hyperelastic membrane component to a linear viscous process. In contrast with the viscous dissipation of energy as heat that occurs in rapid extension of a viscoelastic solid, or in plastic flow of a material above yield, the viscous process in this case represents dissipation produced by permanent molecular reorganization through relaxation of structural membrane components. Data from these experiments determine a characteristic time constant for force relaxation, τ, which is the ratio of a surface viscosity, η to the elastic shear modulus, μ. Because it was found that the concentration of albumin in the cell suspension strongly mediates the rate of force relaxation, values for τ of 10.1, 40.0, 62.8, and 120.7 min are measured at albumin concentrations of 0.0, 0.01, 0.1, and 1.% by weight in grams, respectively. The surface viscosity, η, is calculated from the product of τ and μ. For albumin concentrations of 0.0, 0.01, 0.1, and 1% by weight in grams, η is equal to 3.6, 14.8, 25.6, and 51.9 dyn s/cm, respectively.

INTRODUCTION

The erythrocyte membrane exhibits a spectrum of material behavior ranging from elastic to viscoelastic to plastic. The elastic behavior of the erythrocyte membrane surface is characterized by two constants: an area compressibility modulus, K, and a shear modulus, μ. The values for these moduli have been measured by several investigators (Hochmuth and Mohandus, 1972; Hochmuth et al., 1973; Evans, 1973 *b*; Evans et al., 1976; Evans and Waugh, 1977; Waugh and Evans, 1979), and, at 25°C, are 450 dyn/cm and 0.004–0.0066 dyn/cm for K and μ, respectively. Because $K >> \mu$, the membrane readily undergoes shear deformation at constant surface area.

Viscoelastic material behavior (time-dependent recovery of membrane extensional deformations) was observed by Hoeber and Hochmuth (1970) for erythrocytes expelled suddenly from micropipettes. Subsequent work by Waugh and Evans (1976), Evans and Hochmuth (1976 *a*), Chien et al. (1978), and Hochmuth et al. (1979) indicates that the intrinsic material time constant for viscoelastic recovery is ~0.1 s at 25°C. With the viscoelastic constitutive relation proposed by Evans and Hochmuth (1976 *a*), the value for the surface viscosity in the solid domain of membrane behavior has been estimated to be $\sim 10^{-3}$ dyn s/cm.

Plastic flow of membranes was produced by Hochmuth et al. (1973) when extracellular fluid shear stresses were used to pull filaments of membrane from erythrocytes attached to glass substrates. Evans and Hochmuth (1976 *b*) analyzed the extensional growth rate of the membrane filaments with a Bingham plastic constitutive model, and calculated a value for the surface viscosity of ~0.01 dyn s/cm.

Permanent deformations or "bumps" were observed by Evans and LaCelle (1975) when erythrocytes were aspirated into micropipettes, held there for time periods in excess of 3–4 min, and then expelled from the micropipette. The dependence of the bump height or residual deformation on the duration of extension was indicated; however, no analysis was attempted.

In the present investigation an experiment similar to that of Evans and LaCelle (1975) is used to study the process of force relaxation and permanent deformation in erythrocyte membrane. The experiment, called the micropipette aspiration experiment, produces permanent membrane deformation in the form of a bump on the cell surface. With the use of a nonlinear constitutive equation in which a hyperelastic membrane component is serially

Dr. Markle's present address is Orange Medical Instruments, 3183-F Airway Avenue, Costa Mesa, CA.
Dr. Evan's present address is the Department of Pathology, University of British Columbia, Vancouver, British Columbia.

coupled to a linear viscous component (Evans and Skalak, 1980), an analysis is developed that predicts the bump height as a function of the magnitude and duration of the membrane extension. A characteristic time constant for force relaxation, τ, is defined by this equation and measured in the micropipette aspiration experiment. From the measured value of τ and the elastic shear modulus μ, the coefficient of the viscous element η is deduced. In addition, a second experiment is developed, the whole-cell-extension experiment, in which permanent deformation is produced by extending an erythrocyte between two micropipettes for varying periods of time. Although no analysis is developed for this experiment it offers some qualitative insight into the force relaxation process.

MATERIALS AND METHODS

Micropipette Aspiration

In the micropipette-aspiration experiment a cell is initially aspirated into a pipette at 100–150 dyn/cm^2 (~1.–1.5 mm H_20). The pressure in the pipette is decreased in increments of 50 dyn/cm^2 until the desired pressure is reached. This procedure is recorded on video tape and analyzed according to the method of Evans (1973 *b*) to determine the shear modulus of the cell membrane. As shown in Fig. 1 (*B*, *C*), the cell is held at a constant pressure for the duration of the experiment, after which it is released from the pipette and the residual bump height measured (Fig. 1 *D*). Movement of the membrane material into the pipette (creep) occurs within the first few minutes after the steady-state aspiration pressure is reached. As a result, L_f, the tongue length just before the cell is released, is always greater than L_o, the tongue length at the moment the steady-state aspiration pressure is reached. This difference is variable and maximally on the order of 10% of L_o. The cessation of material movement up the pipette is attributed to frictional interaction and surface adhesion between the cell membrane and the pipette wall. For experiments of long duration the residual bump height is scaled with respect to L_f and plotted as a function of the period of time that the cell is held in the pipette. When the experimental duration is on the order of the creep duration, the average of L_f and L_o is used to scale the bump height. To assess the effects of albumin concentration on the rate at which the permanent deformation (residual bump height) occurs, experiments at four different albumin concentrations (0.0, 0.01, 0.1, and 1.% by weight in grams, see Fig. 2) are performed.

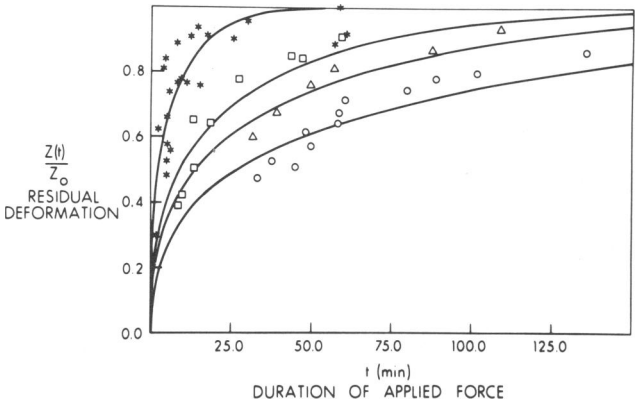

FIGURE 2 Results of the micropipette-aspiration experiment. The residual deformation is defined as the bump height produced after t minutes of aspiration, $Z(t)$, scaled by the length of the cells projection into the pipette, Z_o. Albumin in percent by weight in grams: *, 0.00; □, 0.01; Δ, 0.10; ○, 1.00. τ, in minutes: *, 10.1; □, 40.0; Δ, 62.8; ○, 120.7.

Whole Cell Extension

Whole cell deformation is produced by aspirating diametrically opposite points on the erythrocyte rim into micropipettes and displacing the pipettes so as to produce a symmetrically extended cell (Fig. 3). The extended cell length is held constant for a predetermined time period after which the cell is released from the pipettes. As shown in Fig. 3, the observations recorded in this experiment are:(*a*) The initial cell diameter, L_o (Fig. 3 *A*). (*b*) The length from one cell projection in the pipette to the other, L_∞ (Fig. 3 *B*). (*c*) The overall length of the cell as a function of the time since release, $L(t)$ (Fig. 3 *C–D*).

A normalized residual deformation term similar to that used for the micropipette aspiration experiments is defined by dividing the change in the overall cell length at time t, $L(t) - L_o$, by the maximum possible length change, $L_\infty - L_o$.

$$\text{Residual deformation} = \frac{L(t) - L_o}{L_\infty - L_o}. \qquad (1)$$

The residual deformation is plotted as a function of the time that the cell is extended between the two pipettes (see Fig. 4).

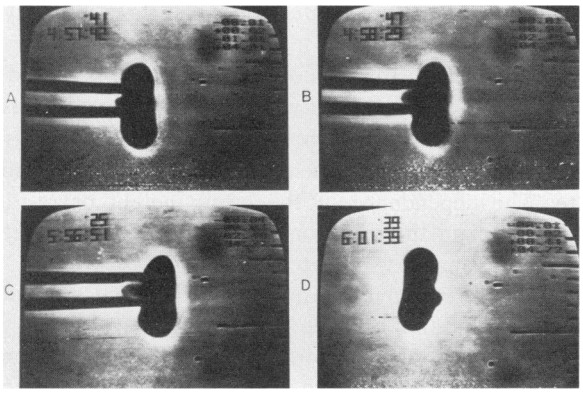

FIGURE 1 Micropipette aspiration experiment. (*A*) Tongue length before complete aspiration. (*B*) Tongue length at the start of the "bump" experiment, L_o. (*C*) Tongue length just before releasing the cell from the pipette, L_f. (*D*) Residual deformation, bump height.

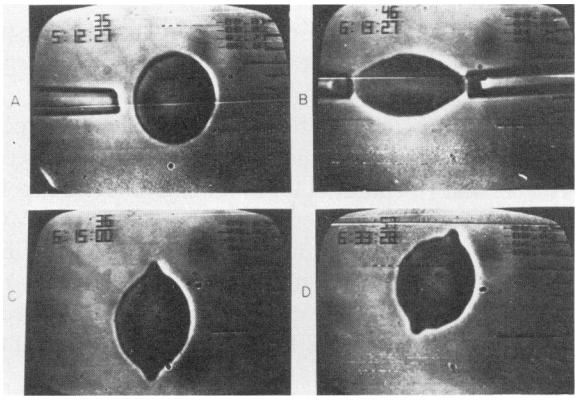

FIGURE 3 Whole-cell-extension experiment. (*A*) The cell just before beginning experiment, L_o. (*B*) The extended cell, L_∞ . (*C*) The cell just after being released, $L(t_o)$. (*D*) The cell ~20 min after being released, $L(t_{20})$.

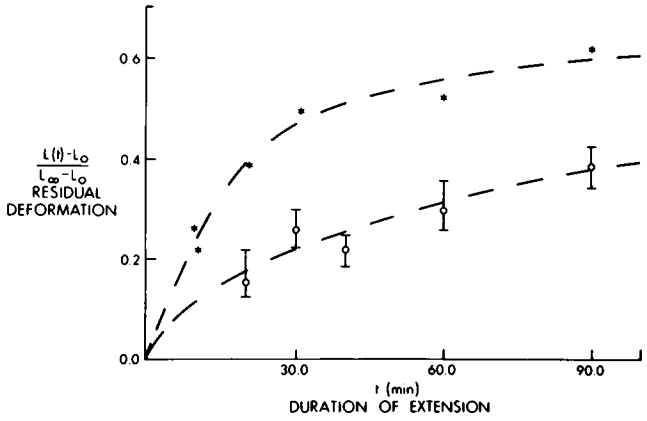

FIGURE 4 Results of the whole-cell-extension experiment. The residual deformation (see Fig. 3 for an explanation of this term) is measured 1 min after the cell is released from both pipettes. *, 0.01% albumin by weight in grams. ○, 1.% albumin by weight in grams.

Solution Preparations

For all experiments, a stock solution of phosphate-buffered saline (PBS) containing 121.5 mM NaCl, 25.2 mM Na_2HPO_4, 4.8 mM KH_2PO_4, 100 units/ml penicillin, and 100 μg/ml streptomycin is mixed and adjusted to a pH of ~7.4 and an osmolarity between 250 and 300 mOsm. Human albumin is then added to a 100 ml sample of the stock solution, and the solution filtered to remove bacteria and debris. Albumin concentrations are selected between 0.0 and 1.0 % by weight in grams while the osmolarity is selected to minimize the depth of the cell dimple without producing cup-shaped cells. The salt and albumin concentrations are not changed in any systematic way and all filtering is done with a Millipore GS-grade filter.

Apparatus

In the micropipette-aspiration experiment only micropipettes with flat tips and inside diameters between 1.1 and 1.4 μm are used. Slightly smaller pipettes are used in the whole-cell-extension experiment. All pipettes are filled by boiling them in PBS in a vacuum. At the start of an experiment, a pipette is mounted in the De Fronbrune micromanipulator and coupled by a continuous water system to a reservoir that was positioned using a micrometer and a Validyne model DP103 pressure transducer (Validyne Engineering Corp. Northridge, CA). The output of the transducer is nulled electronically. To obtain a null pressure in the pipette while the transducer null point is maintained, the relative positions of the reservoir and transducer are fixed. In effect they form a coupled unit. Vertical adjustment of this unit alongside the pipette adjusts the pipette pressure without changing the transducer null point. The pipette null pressure is detected by observing the movement of an erythrocyte placed in front of the pipette. When the cell remains stationary there is no flow of fluid into or out of the pipette. This procedure establishes the pipette null pressure to within ±10 dyn/cm² (10^{-5} atm). Maintenance of a small positive pressure in the cell chamber and placement of an insulated box around the microscope stage limits drift of the null pressure to $< \pm 10$ dyn/cm². Without this small positive pressure, evaporation from the cell chamber changes the curvature of the air-water interface, and thus the pressure in the cell chamber. The insulated box eliminates transient temperature changes resulting from thermal convection.

A Leitz inverted microscope and appropriate video recording, mixing, and enhancing devices are used to allow simultaneous visual observation and recording of experiments. During an experiment the erythrocytes are contained in a temperature-controlled chamber similar to the one described by Waugh and Evans (1979) but modified to allow rapid infusion of cell suspensions into the chamber without the removal of either the chamber from the microscope or the pipettes from the chamber. For details of this modification see Markle (1980).

ANALYSIS

No analysis of the whole-cell-extension experiment is attempted due to the asymmetry of the surface deformations. However, for the axisymmetric surface deformation produced in the micropipette aspiration experiment, an analysis is developed to evaluate the force relaxation time constant. This requires that the measurable parameters of the experiment, i.e., the length of the cell projection into the pipette, the duration of the applied force, and the residual bump height, be related to the intrinsic parameters of an appropriate constitutive equation. The constitutive equation used was developed by Evans and Skalak (1980) from a finite deformation Maxwell model for a material that is incompressible in two dimensions. Because they present a thorough development of the constitutive equation only a brief discussion is given here.

By definition, a Maxwell model is a serial coupling of an elastic and viscous element. For two such elements in series the total rate of deformation is equal to the sum of the deformation rates of the individual elements. However, since a material that is incompressible in two dimensions can experience only shear deformation, the total rate of deformation is the total rate of shear deformation, and is equal to the sum of the rate of shear deformation in the elastic and viscous elements, V_s^e and V_s^v.

$$V_s = V_s^e + V_s^v. \tag{2}$$

As shown by Evans and Skalak (1980) the shear resultant V_s may be expressed as the time rate of change of the logarithm of the principal extension ratio $\tilde{\lambda}$

$$V_s = \frac{\partial \ln \tilde{\lambda}}{\partial t}. \tag{3}$$

Thus Eq. 2 may be written as

$$\frac{\partial \ln \tilde{\lambda}}{\partial t} = \frac{\partial \ln \tilde{\lambda}_e}{\partial t} + \frac{\partial \ln \tilde{\lambda}_v}{\partial t} \tag{4}$$

or

$$\tilde{\lambda} = \tilde{\lambda}_e \lambda_v \tag{5}$$

where $\tilde{\lambda}$ is the overall principal extension ratio, and $\tilde{\lambda}_e$ and $\tilde{\lambda}_v$ are extension ratios conceptually associated with the elastic and viscous elements of the Maxwell model. Note that $\tilde{\lambda}_v$ is a measure of permanent deformation which results from force relaxation, while $\tilde{\lambda}_e$ is a measure of the recoverable or elastic deformation. In their model Evans and Skalak assume that the elastic element of the model behaves according to the elastic constitutive equation for erythrocyte membrane (Evans, 1973 *a*),

$$T_s = \frac{\mu}{2}(\tilde{\lambda}_e^2 - \tilde{\lambda}_e^{-2}), \tag{6}$$

while the viscous element behaves according to Newton's law of viscosity:

$$T_s = 2\eta V_s^v. \tag{7}$$

(Note that T_s is the maximum shear resultant, μ is the elastic shear modulus, and η is a surface viscosity.) Thus the desired constitutive relation is obtained by combining Eqs. 4, 6, and 7,

$$\frac{\partial \ln \tilde{\lambda}}{\tilde{t}} = \frac{1}{2\sqrt{\tilde{T}_S^2 + 1}} \frac{\partial \tilde{T}_S}{\tilde{t}} + \frac{\tilde{T}_S}{2}, \tag{8}$$

where the dimensionless shear-stress resultant, $\tilde{T}_s$ and time $\tilde{t}$ are $\tilde{T}_s = T_s/\mu$ and $\tilde{t} = t/(\eta/\mu)$.

To use this constitutive equation in the analysis of the micropipette aspiration experiment, the following assumptions and approximations are made:

(*a*) The area of the membrane is assumed constant throughout the deformation process. Because the area compressibility modulus is over four orders of magnitude greater than the shear modulus, no significant area dilation occurs for the force levels used in these measurements.

(*b*) The membrane is modeled as a flat plane of infinite extent (no tensions at the boundaries) that is deformed into a cylinder with a hemispherical cap (Evans, 1973 *b*). From the elastic constitutive equation and the constant area assumption, it has been shown that the elastic shear resultant decreases as the square of the distance from the axis of symmetry (Evans, 1973 *b*). Because the average erythrocyte diameter is eight μm and the average diameter of the pipette is 1.2 μm, the shear resultant at the cell edge is ~2% of its value at the pipette base. Thus, for cells aspirated in the dimple region, the infinite-plane assumption is reasonable. Fig. 5 shows the geometric model used in the analysis and a schematic representation of the aspiration of an erythrocyte into a micropipette.

(*c*) The aspirated tongue length is considered to be constant for the duration of the experiment. This assumption is based on the observation that movement of material up the pipette ceases shortly after the beginning of the experiment, and results in only a small increase in the initial tongue length, i.e., 5–10% of L_o. The cessation of movement is attributed to adhesion of the cell to the pipette wall.

Based on these assumptions, an analysis is developed to predict the height and shape of a bump left on an infinite plane of material after the plane is partially aspirated into a pipette, held for a variable period of time, and released. The analysis is divided into three steps:(*a*) determination of the extension ratio $\tilde{\lambda}$ along the undeformed radial coordinate r_o, see Fig. 5; (*b*) determination of the plastic (residual) extension ratio distribution, $\tilde{\lambda}_v(r_o)$, as a function of the duration of an experiment; and (*c*) determination of the residual bump height and shape from $\tilde{\lambda}(r_o)$.

Initial Extension Ratio. The extension ratio, $\tilde{\lambda}$, for an axisymmetric and planar deformation is given by the ratio of the width of a deformed annular ring to its width before deformation (see Fig. 5).

$$\tilde{\lambda} = \frac{dr}{dr_o}. \tag{9}$$

Because the area of an annular ring must remain constant during deformation ($2\pi r_o dr_o = 2\pi r dr$), $\tilde{\lambda}$ is also the ratio of the initial to final radius of the annular ring.

$$\tilde{\lambda} = \frac{dr}{dr_o} = \frac{r_o}{r}. \tag{10}$$

To determine $\tilde{\lambda}(r_o)$ the material in the pipette is divided into two regions (see Fig. 5): the hemispherical cap ($0 < Z < R_p$), and the cylindrical section ($R_p < Z < L$). The deformation in each region is then considered separately.

For the hemispherical cap, conservation of area requires that the area of the cap, A_{cap}, be equal to the area occupied by the cap material in the undeformed plane:

$$\pi r_o^2 = A_{cap}. \tag{11}$$

With A_{cap} expressed in terms of the pipette radius, R_p, and the deformed radial coordinate, r, [$A_{cap} = 2\pi R_p (R_p - \sqrt{R_p^2 - r^2})$] Eq. 11 can be rewritten to specify $\tilde{\lambda}(r_o)$ as follows:

$$\lambda(r_o) = \left(\frac{4R_p^2}{4R_p^2 - r_o^2}\right)^{1/2} \cdot 0 < r_o < R_p\sqrt{2}. \tag{12}$$

For the cylindrical section, $R_p < Z < L$, the deformed radial coordinate, r, is constant and equal to R_p. Thus a substitution of R_p for r in Eq. 10

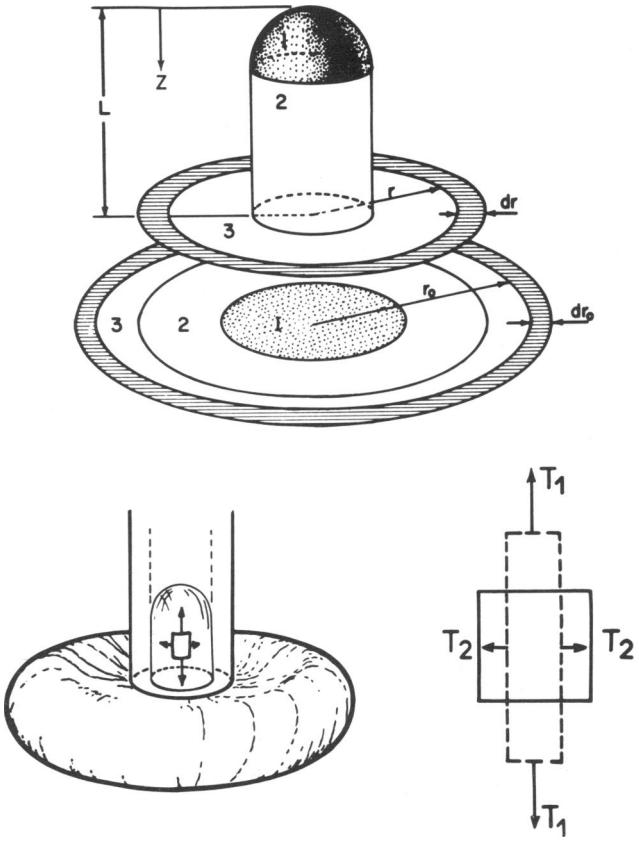

FIGURE 5 A schematic illustration of the aspiration of an erythrocyte into a micropipette, and the geometric model used in the analysis. Shaded areas have equal areas (taken from Waugh and Evans, 1979).

defines $\tilde{\lambda}$ along the cylindrical section as follows:

$$\tilde{\lambda} = \frac{r_o}{R_p} \cdot R_p < Z < L \tag{13}$$

The Residual Extension Ratio, $\tilde{\lambda}_v(r_o)$. When the rate of material deformation is zero the constitutive equation becomes

$$\frac{\partial \ln\tilde{\lambda}}{\partial \tilde{t}} \equiv 0 \equiv \frac{1}{2\sqrt{\tilde{T}_s^2 + 1}} \frac{\partial \tilde{T}_s}{\partial \tilde{t}} + \frac{\tilde{T}_s}{2}. \tag{14}$$

A substitution of $1/2(\tilde{\lambda}^2 - \tilde{\lambda}^{-2})$ for $\tilde{T}_s$ in Eq. 14 (see Eq. 6) results in a differential equation integrable by separation of variables. Evaluation of this integral between the limits of $\tilde{\lambda}_v(\tilde{t} = 0)$ and $\tilde{\lambda}_e(\tilde{t})$ yields the following relation:

$$e^{-\tilde{t}}\left(\frac{\tilde{\lambda}^2 - 1}{\tilde{\lambda}^2 + 1}\right) = \left(\frac{\tilde{\lambda}_e^2 - 1}{\tilde{\lambda}_e^2 + 1}\right). \tag{15}$$

Note that at $\tilde{t} = 0$ no relaxation has occurred, i.e., $\tilde{\lambda}_e(t = 0) = \tilde{\lambda}$. With a further substitution of $\tilde{\lambda}/\tilde{\lambda}_v$ for $\tilde{\lambda}_e$ in Eq. 15 (see Eq. 5), the desired relation between $\tilde{\lambda}$, $\tilde{\lambda}_v$, and $\tilde{t}$ is obtained.

$$e^{-\tilde{t}}\left(\frac{\tilde{\lambda}^2 - 1}{\tilde{\lambda}^2 + 1}\right) = \left(\frac{\tilde{\lambda}^2 - \tilde{\lambda}_v^2}{\tilde{\lambda}^2 + \tilde{\lambda}_v^2}\right). \tag{16}$$

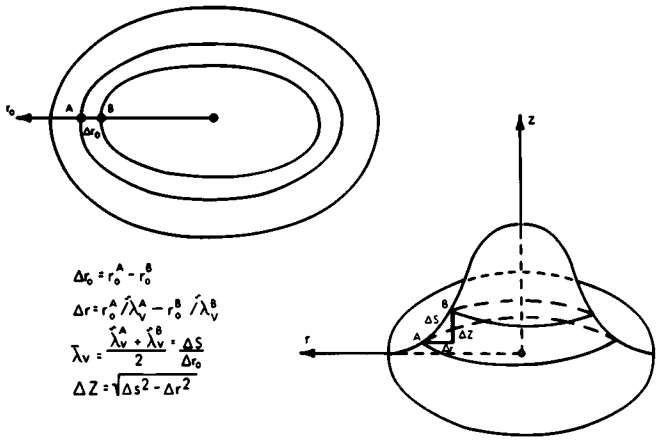

FIGURE 6 Schematic illustration of the deformation of a flat plane into a bump. The undeformed annular ring and the conical annular ring on the bump surface have equal area.

Thus as $\tilde{t} \to \infty$, $\tilde{\lambda}_e \to 1$ and $\tilde{\lambda}_v \to \tilde{\lambda}$, i.e., permanent deformation is produced.

Residual Bump Height

Initially the undeformed membrane plane is conceptually divided into a series of concentric annular rings, each of width Δr_o (see Fig. 6). Because the deformation of the plane into a bump is axisymmetric, each ring forms a conical annulus as it is mapped onto the bump surface. For the deformation of a flat annular ring of differential width, dr_o, into a frustum of meridional length, ds, the ratio ds/dr_o defines the extension ratio, $\tilde{\lambda}_v$:

$$\tilde{\lambda}_v = \frac{ds}{dr_o}. \tag{17}$$

However, for the deformation of a flat annular ring of finite width, Δr_o, into a frustum of finite meridional length, Δs, the ratio $\Delta s/\Delta r_o$ is not a single extension ratio but is an average of the $\tilde{\lambda}_v$ distribution along the annular ring width, Δr_o. For sufficiently small values of Δr_o this ratio is approximated as

$$\Delta s/\Delta r_o = \Delta s/[r_o(j) - r_o(j-1)] = [\tilde{\lambda}_v(j) + \tilde{\lambda}_v(j-1)]/2. \tag{18}$$

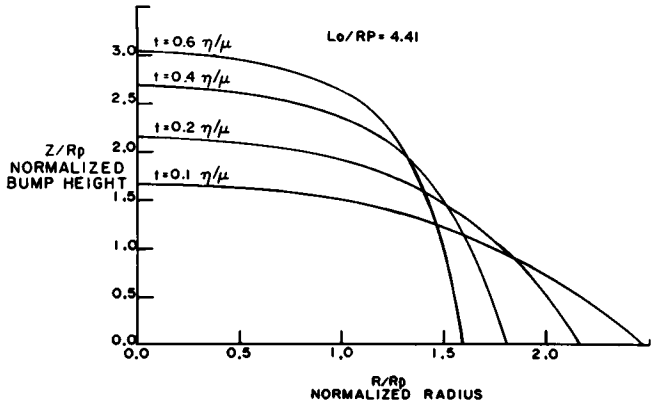

FIGURE 7 Analytically predicted bump shapes for several values of time $\tilde{t}$. The initial tongue length, L_o, is constant for each curve and both the bump height, Z, and radial coordinate, R, are scaled by the pipette radius, R_p.

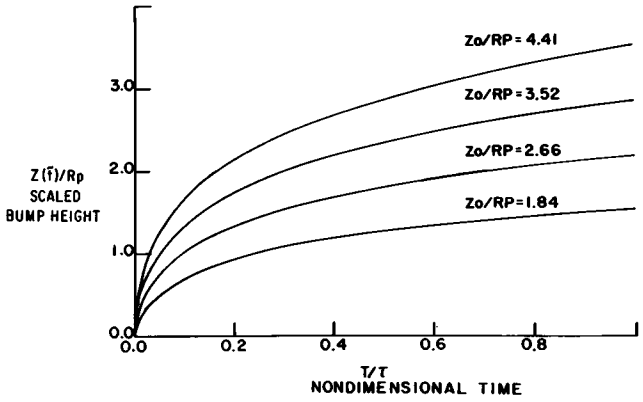

FIGURE 8 Analytical prediction of the scaled bump height, $Z(t)/R_p$, which is produced after $t/\tau = \tilde{t}$ units of nondimensional time. Note that for each curve the initial tongue length in the pipette, Z_o/R_p, is fixed ($\partial \ln \tilde{\lambda}/\partial \tilde{\tau} \equiv 0$) so that no creep up the pipette occurs.

With this approximation and the known variation of $\tilde{\lambda}_v$ with r_o, Δs is determined for each annular ring in the undeformed plane. To obtain the projection of Δs onto the radial coordinate axis, r, i.e., Δr (see Fig. 6) both the constant area assumption, $\tilde{\lambda}_v = r_o/r$, and the variation of $\tilde{\lambda}_v$ with r_o are used:

$$\Delta r = [r_o(j)/\tilde{\lambda}_v(j)] - [r_o(j-1)/\tilde{\lambda}_v(j-1)]. \tag{19}$$

Once Δr and Δs are known for each annular ring, the contribution of each ring to the bump height, ΔL, is calculated using the pythagorean theorem,

$$\Delta L = \sqrt{\Delta s^2 - \Delta r^2}, \tag{20}$$

and summed to predict the bump height. (Note the bump shape can also be approximated by plotting Δr vs. ΔL for each annular ring.)

Results of the Analysis

With the preceding analysis both bump shapes and heights are predicted as a function of the dimensionless time $\tilde{t}$, and the scaled tongue length, L_o/R_p. In Fig. 7, a typical set of bump shapes (for a specific tongue length) are shown as a function of $\tilde{t}$, while in Fig. 8 the bump height as a function of $\tilde{t}$ is plotted for several values of L_o/R_p. When the curves in Fig. 8 are normalized by their respective values of L_o/R_p the results can be approximated by a single curve (see Fig. 9). Because over the range of

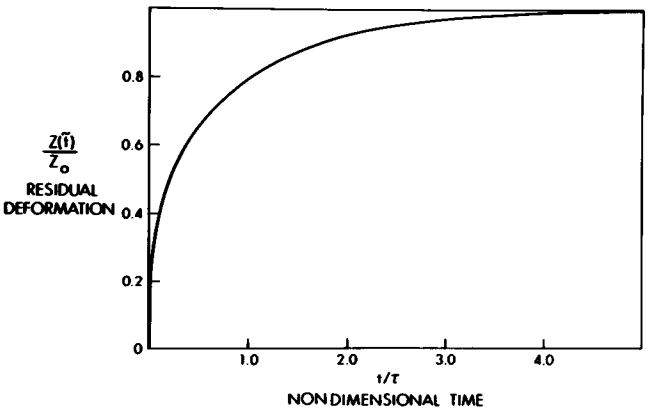

FIGURE 9 Analytically predicted residual deformation, $Z(\tilde{t})/Z_o$, after $t/\tau = \tilde{t}$ units of nondimensional time.

L_o/R_p values produced in the bump experiment (2.–3.0) the difference between the normalized curves is maximally 1%, Fig. 9 is used to reduce all the data. (Note the uncertainty in the experimental measurements is on the order of 10–15%; thus, the error introduced by using Fig. 9 for all data reduction is insignificant.

RESULTS

Micropipette Aspiration

In Fig. 2, the residual height of each bump is shown scaled by its initial tongue length, and plotted as a function of the duration of the experiment. The data shown are from experiments at four concentrations of albumin in the suspending medium. The solid curves are a least-squares fit of the theoretical curve (Fig. 9) to the data taken at each albumin concentration. From these curves a characteristic time constant for force relaxation (permanent deformation), τ, is determined. These values indicate that an increase in the albumin concentration from 0.0 to 1.% by weight in grams increases τ by more than an order of magnitude. Because τ is equal to η/μ and measurements indicate that μ is not a function of albumin concentration (see Table I), η must increase dramatically as the concentration of albumin in the suspending medium is increased.

Whole Cell Extension

Just as in the micropipette aspiration experiments, the time constant for force relaxation in these experiments (Fig. 4) increases with increasing concentration of albumin in the suspending medium. Because large areas of the cell are not in contact with the glass surface, this suggests that an interaction at the cell membrane–glass wall interface is not the sole cause of permanent deformation in the membrane. However, since small areas of the cell membrane are in contact with glass such an interaction cannot be ruled out. It is interesting to note that if permanent deformation occurs only in areas contacted by glass, the deformed cell shape should be an approximate discocyte with two bumps on its rim, whereas if force relaxation occurs over the entire cell surface the deformed cell should be lemon or football shaped. However, because it is not known whether any glass effect on the cell membrane may be transmitted from the contact area to the parts of the membrane that are not in contact with the glass, caution must be used in concluding that the lemon shape is an indication of non–glass-induced force relaxation.

TABLE I
EXPERIMENTALLY DETERMINED VALUES OF THE FORCE RELAXATION TIME CONSTANT, τ, AND THE ELASTIC SHEAR MODULUS, μ, AS A FUNCTION OF ALBUMIN CONCENTRATION

Albumin concentration (percent by weight in grams)	τ	$\bar{\mu}10^{-3}$	$\bar{\eta}$
	min	*dyn/cm*	*dyn s/cm*
0.0	10.1	5.97	3.61
0.01	40.0	6.20	14.88
0.10	62.8	6.83	25.62
1.0	120.7	7.17	51.9

The viscous coefficient, η, is deduced from the values of τ and μ.

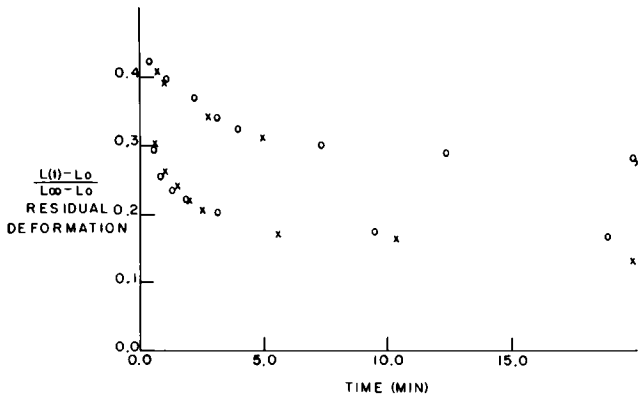

FIGURE 10 Data from the whole-cell-extension experiment illustrating the independence of the recovery process from the concentration of albumin in the suspending medium. x, 0.01% by weight in grams; o, 1.% by weight in grams.

One other observation made in the whole-cell-extension experiment is that after the release of a cell from the two pipettes, the length of the cell, i.e., the distance between the two bumps on the cell rim, decreases over a period of minutes. This is shown in the photographs in Fig. 3 *C–D*, where a cell is shown just after its release from the pipettes and again 20 min later. In Fig. 10 this "recovery" process is represented by the plot of a cells' residual deformation (see Eq. 1) as a function of the time since its release. Two pairs of curves, one at an initial residual deformation of ~0.4 and the other at an initial residual deformation of ~0.3, are presented in Fig. 10. Each pair represents the recovery of one cell at 0.01% by weight in grams albumin and another cell 1.0% by weight in grams albumin. From these results it appears that the concentration of albumin in the suspending medium does not affect the recovery process. (Note that the duration of the extension required to produce the initial residual deformations, 0.4 or 0.3, are shown in Fig. 4.)

DISCUSSION

In both micropipette aspiration and whole-cell-extension experiments, albumin in the suspending medium mediates the rate of force relaxation in erythrocyte membrane. In the micropipette-aspiration experiment, this is reflected in the measured value of the characteristic time constant for force relaxation, while in the whole-cell-extension experiment it is qualitatively apparent. However, there are two major differences between the results of these experiments:

(*a*) In the whole cell extension experiment, a significant amount of recovery is measured, while in the micropipette

aspiration experiment, only a small amount of recovery is observed. The one exception occurs with bumps formed by aspiration of a cell to a maximum extension ratio of 2:1 or 3:1 and held for a short period of time. These bumps recover significantly with time, and are often completely reabsorbed into the cell body.

(*b*) In the micropipette aspiration experiment the residual deformation term (Fig. 2) always approaches unity, i.e., a totally relaxed geometry, while in the whole-cell-extension experiment the residual deformation parameter (Eq. 1) appears to approach a value less than unity.

These discrepancies can be resolved if it is assumed that the characteristic time constant for force relaxation, τ, is a function of extension. To illustrate this, assume τ is significantly greater for extension ratios <1.5 than for extension ratios >3. Then, in the whole-cell-extension experiment where the center region of the cell is slightly extended ($\tilde{\lambda} <$ 1.5) and the two end regions significantly extended ($\tilde{\lambda} >$ 2.5), deformations maintained for a period of time equal to the "end region" time constant will produce cells with significantly relaxed end regions and a slightly relaxed center region, while deformations maintained for a period of time equal to the "center region" time constant will produce cells with totally relaxed end regions and a partially relaxed center region. As a result, cells released from the pipettes after an end region time constant will exhibit whole cell recovery as the center region pulls the ends towards the middle. Also, the quick relaxation of the end regions will produce a fast rise in the residual deformation curve (Fig. 4), while the slow relaxation of the center region will govern the approach of the residual deformation to unity. All of these effects are seen in the data obtained from the whole cell extension experiments.

Likewise, in the micropipette aspiration experiment where the area around the base of the pipette is significantly extended and the remainder of the cell surface slightly extended, bumps produced in a "base" time constant or less will be partially pulled back into the cell surface by the unrelaxed area in the plane of the membrane. However, once the base material has totally relaxed, the balance of the material in the pipette will be "caught" above this region. Thus the relaxation rate of the base material will dominate the rate of bump formation and the residual deformation term (Fig. 2) will approach unity with an apparent single time constant.

The existence of this type of nonlinear material has precedence in the literature. In 1978, Chien et al. reported an extension-dependent time constant for viscoelastic material behavior of erythrocytes. Although their time constants were much shorter (0.018–0.115 s) than those reported here, their findings support the proposal that the time constant for force relaxation may be a function of extension.

The observation that the presence of albumin in the suspending medium mediates the rate of bump formation suggests that the albumin is either altering the intrinsic material properties of the cell membrane or is mediating a process, such as glass–cell membrane interaction, which is at least partially responsible for the formation of bumps. In support of this latter possibility are the adsorption isotherms of albumin to silica (Morrissey and Stromberg, 1974) and to erythrocyte membrane (Janzen and Brooks, personal communication). For erythrocyte membrane, the adsorption isotherm at 25°C is linear to 5 g/100 ml and at 1 g/100 ml has an upper limit of $5 \times 10^{-6} \pm 5 \times 10^{-6}$ molecules/A^{o2}. For silica the adsorption isotherm at 23°C asymptotically approaches a saturation density of 7.8×10^{-5} molecules/A^{o2} at 1 g/100 ml. For an assumed erythrocyte area of 140 μm^2 the ratio of adsorbed albumin on silica to that adsorbed on erythrocyte membrane is ~16:1 at 1 g/100 ml and 111:1 at 0.1 g/100 ml. This ratio continues to increase as the albumin concentration decreases, indicating that albumin at a cell membrane–glass wall interface is primarily associated with glass and not cell membrane. Furthermore, by assuming an albumin saturation density on the erythrocyte membrane similar to that found on silica (7.8×10^{-5} molecules/A^{o2}), the percentage of erythrocyte membrane covered by the adsorbed albumin at 1 g/100 ml is only 6.6%. Thus it appears unlikely that enough albumin is adsorbed to the erythrocyte membrane to effect the measured change in the force relaxation time constant. It is also noteworthy that a graph of τ vs. albumin concentration is very similar in shape to the adsorption isotherm of albumin to silica.

In summary, it appears that the albumin present at a cell membrane–glass wall interface is associated primarily with the glass surface and is not present on the membrane surface in sufficient quantities to significantly alter the intrinsic material properties of the cell membrane. In light of this information and the results of the micropipette aspiration experiment the existance of an albumin-mediated glass effect is highly suspect. In addition, the discrepancies between the micropipette-aspiration and whole-cell-extension experiments can be resolved by assuming that the characteristic time constant for force relaxation is a function of extension. Because there are other possible explanations for these discrepancies and for the results of the micropipette-aspiration experiments, more definitive experiments are needed—perhaps ones that do not involve a glass surface.

This work was supported by National Institutes of Health grant HL 23728 and HL 16711.

Received for publication 1 December 1981 and in final form 7 June 1982.

REFERENCES

Chien, S. K., L. P. Sung, R. Skalak, S. Usami, and A. Tozeren. 1978. Theoretical and experimental studies on viscoelastic properties of erythrocyte membrane. *Biophys. J.* 24:463–487.

Evans, E. A. 1973 *a*. A new material concept for the red cell membrane. *Biophys. J.* 13:926–940.

Evans, E. A. 1973 *b*. New membrane concept applied to the analysis of fluid-shear and micropipette-deformed erythrocytes. *Biophys. J.* 13:941–954.

Evans, E. A., and R. M. Hochmuth. 1976 *a*). Membrane viscoelasticity. *Biophys. J.* 16:1–11.

Evans, E. A., and R. M. Hochmuth. 1976 *b*. Membrane viscoplastic flow. *Biophys. J.* 16:13–26.

Evans, E. A., and P. L. LaCelle. 1975. Intrinsic material properties of the erythrocyte membrane indicated by mechanical analysis of the deformation. *Blood.* 45:29–43.

Evans, E. A., and R. Skalak. 1980. Mechanics and thermodynamics of biomembranes. CRC Press, Inc., Boca Raton, FL.

Evans, E. A., R. Waugh, and L. Melnik. 1976. Elastic area compressibility modulus of red cell membrane. *Biophys. J.* 16:585–595.

Evans, E. A., and R. Waugh. 1977. Osmotic correction to elastic area compressibility measurements on cell membrane. *Biophys. J.* 20:307–313.

Hochmuth, R. M., and N. Mohandus. 1972. Uniaxial loading of the cell membrane. *J. Biomech.* 5:501.

Hochmuth, R. M., N. Mohandus, and P. L. Blackshear, Jr. 1973. Measurement of the elastic modulus for red cell membrane using a fluid mechanical technique. *Biophys. J.* 13:747–762.

Hochmuth, R. M., P. R. Worthy, and E. A. Evans. 1979. Red cell extensional recovery and the determination of membrane viscosity. *Biophys. J.* 26:101–114.

Hoeber, T. W., and R. M. Hochmuth. 1970. Measurement of red cell modulus of elasticity by in-vitro and model cell experiments. *Trans. A..M.E. J. Basic Eng.* 92:604.

Markle, D. R. 1980. Force relaxation and permanent deformation of red cell membrane. Ph.D. Dissertation, Duke University, Durham, NC.

Morrissey, B. W., and R. R. Stromberg. 1974. The conformation of adsorbed blood proteins by infrared bound fraction measurements. *J. Colloid Interface Sci.* 46:152–154.

Waugh, R. E. 1977. Temperature dependence of the elastic properties of red blood cell membrane. Ph.D. Dissertation, Duke University, Durham, NC.

Waugh, R., and E. A. Evans. 1976. Viscoelastic properties of erythrocyte membrane of different vertebrate animals. *Microvasc. Res.* 12:291.

Waugh, R., and E. A. Evans. 1979. Thermoelasticity of erythrocyte membrane. *Biophys. J.* 26:115–131.